August 2008
hep-ex/arXiv:0808.1838
SLAC-PUB-13352
BABAR-PUB-08/032

Measurement of the Branching Fractions of the Radiative Charm Decays $D^0 \to \bar{K}^{*0}\gamma$ and $D^0 \to \phi\gamma$

B. Aubert,[1] M. Bona,[1] Y. Karyotakis,[1] J. P. Lees,[1] V. Poireau,[1] E. Prencipe,[1] X. Prudent,[1] V. Tisserand,[1] J. Garra Tico,[2] E. Grauges,[2] L. Lopez[ab],[3] A. Palano[ab],[3] M. Pappagallo[ab],[3] G. Eigen,[4] B. Stugu,[4] L. Sun,[4] G. S. Abrams,[5] M. Battaglia,[5] D. N. Brown,[5] R. N. Cahn,[5] R. G. Jacobsen,[5] L. T. Kerth,[5] Yu. G. Kolomensky,[5] G. Lynch,[5] I. L. Osipenkov,[5] M. T. Ronan,[5,*] K. Tackmann,[5] T. Tanabe,[5] C. M. Hawkes,[6] N. Soni,[6] A. T. Watson,[6] H. Koch,[7] T. Schroeder,[7] D. Walker,[8] D. J. Asgeirsson,[9] B. G. Fulsom,[9] C. Hearty,[9] T. S. Mattison,[9] J. A. McKenna,[9] M. Barrett,[10] A. Khan,[10] V. E. Blinov,[11] A. D. Bukin,[11] A. R. Buzykaev,[11] V. P. Druzhinin,[11] V. B. Golubev,[11] A. P. Onuchin,[11] S. I. Serednyakov,[11] Yu. I. Skovpen,[11] E. P. Solodov,[11] K. Yu. Todyshev,[11] M. Bondioli,[12] S. Curry,[12] I. Eschrich,[12] D. Kirkby,[12] A. J. Lankford,[12] P. Lund,[12] M. Mandelkern,[12] E. C. Martin,[12] D. P. Stoker,[12] S. Abachi,[13] C. Buchanan,[13] J. W. Gary,[14] F. Liu,[14] O. Long,[14] B. C. Shen,[14,*] G. M. Vitug,[14] Z. Yasin,[14] L. Zhang,[14] V. Sharma,[15] C. Campagnari,[16] T. M. Hong,[16] D. Kovalskyi,[16] M. A. Mazur,[16] J. D. Richman,[16] T. W. Beck,[17] A. M. Eisner,[17] C. J. Flacco,[17] C. A. Heusch,[17] J. Kroseberg,[17] W. S. Lockman,[17] A. J. Martinez,[17] T. Schalk,[17] B. A. Schumm,[17] A. Seiden,[17] M. G. Wilson,[17] L. O. Winstrom,[17] C. H. Cheng,[18] D. A. Doll,[18] B. Echenard,[18] F. Fang,[18] D. G. Hitlin,[18] I. Narsky,[18] T. Piatenko,[18] F. C. Porter,[18] R. Andreassen,[19] G. Mancinelli,[19] B. T. Meadows,[19] K. Mishra,[19] M. D. Sokoloff,[19] P. C. Bloom,[20] W. T. Ford,[20] A. Gaz,[20] J. F. Hirschauer,[20] M. Nagel,[20] U. Nauenberg,[20] J. G. Smith,[20] K. A. Ulmer,[20] S. R. Wagner,[20] R. Ayad,[21,†] A. Soffer,[21,‡] W. H. Toki,[21] R. J. Wilson,[21] D. D. Altenburg,[22] E. Feltresi,[22] A. Hauke,[22] H. Jasper,[22] M. Karbach,[22] J. Merkel,[22] A. Petzold,[22] B. Spaan,[22] K. Wacker,[22] M. J. Kobel,[23] W. F. Mader,[23] R. Nogowski,[23] K. R. Schubert,[23] R. Schwierz,[23] A. Volk,[23] D. Bernard,[24] G. R. Bonneaud,[24] E. Latour,[24] M. Verderi,[24] P. J. Clark,[25] S. Playfer,[25] J. E. Watson,[25] M. Andreotti[ab],[26] D. Bettoni[a],[26] C. Bozzi[a],[26] R. Calabrese[ab],[26] A. Cecchi[ab],[26] G. Cibinetto[ab],[26] P. Franchini[ab],[26] E. Luppi[ab],[26] M. Negrini[ab],[26] A. Petrella[ab],[26] L. Piemontese[a],[26] V. Santoro[ab],[26] R. Baldini-Ferroli,[27] A. Calcaterra,[27] R. de Sangro,[27] G. Finocchiaro,[27] S. Pacetti,[27] P. Patteri,[27] I. M. Peruzzi,[27,§] M. Piccolo,[27] M. Rama,[27] A. Zallo,[27] A. Buzzo[a],[28] R. Contri[ab],[28] M. Lo Vetere[ab],[28] M. M. Macri[a],[28] M. R. Monge[ab],[28] S. Passaggio[a],[28] C. Patrignani[ab],[28] E. Robutti[a],[28] A. Santroni[ab],[28] S. Tosi[ab],[28] K. S. Chaisanguanthum,[29] M. Morii,[29] A. Adametz,[30] J. Marks,[30] S. Schenk,[30] U. Uwer,[30] V. Klose,[31] H. M. Lacker,[31] D. J. Bard,[32] P. D. Dauncey,[32] J. A. Nash,[32] M. Tibbetts,[32] P. K. Behera,[33] X. Chai,[33] M. J. Charles,[33] U. Mallik,[33] J. Cochran,[34] H. B. Crawley,[34] L. Dong,[34] W. T. Meyer,[34] S. Prell,[34] E. I. Rosenberg,[34] A. E. Rubin,[34] Y. Y. Gao,[35] A. V. Gritsan,[35] Z. J. Guo,[35] C. K. Lae,[35] N. Arnaud,[36] J. Béquilleux,[36] A. D'Orazio,[36] M. Davier,[36] J. Firmino da Costa,[36] G. Grosdidier,[36] A. Höcker,[36] V. Lepeltier,[36] F. Le Diberder,[36] A. M. Lutz,[36] S. Pruvot,[36] P. Roudeau,[36] M. H. Schune,[36] J. Serrano,[36] V. Sordini,[36,¶] A. Stocchi,[36] G. Wormser,[36] D. J. Lange,[37] D. M. Wright,[37] I. Bingham,[38] J. P. Burke,[38] C. A. Chavez,[38] J. R. Fry,[38] E. Gabathuler,[38] R. Gamet,[38] D. E. Hutchcroft,[38] D. J. Payne,[38] C. Touramanis,[38] A. J. Bevan,[39] C. K. Clarke,[39] K. A. George,[39] F. Di Lodovico,[39] R. Sacco,[39] M. Sigamani,[39] G. Cowan,[40] H. U. Flaecher,[40] D. A. Hopkins,[40] S. Paramesvaran,[40] F. Salvatore,[40] A. C. Wren,[40] D. N. Brown,[41] C. L. Davis,[41] A. G. Denig,[42] M. Fritsch,[42] W. Gradl,[42] G. Schott,[42] K. E. Alwyn,[43] D. Bailey,[43] R. J. Barlow,[43] Y. M. Chia,[43] C. L. Edgar,[43] G. Jackson,[43] G. D. Lafferty,[43] T. J. West,[43] J. I. Yi,[43] J. Anderson,[44] C. Chen,[44] A. Jawahery,[44] D. A. Roberts,[44] G. Simi,[44] J. M. Tuggle,[44] C. Dallapiccola,[45] X. Li,[45] E. Salvati,[45] S. Saremi,[45] R. Cowan,[46] D. Dujmic,[46] P. H. Fisher,[46] G. Sciolla,[46] M. Spitznagel,[46] F. Taylor,[46] R. K. Yamamoto,[46] M. Zhao,[46] P. M. Patel,[47] S. H. Robertson,[47] A. Lazzaro[ab],[48] V. Lombardo[a],[48] F. Palombo[ab],[48] J. M. Bauer,[49] L. Cremaldi,[49] R. Godang,[49,**] R. Kroeger,[49] D. A. Sanders,[49] D. J. Summers,[49] H. W. Zhao,[49] M. Simard,[50] P. Taras,[50] F. B. Viaud,[50] H. Nicholson,[51] G. De Nardo[ab],[52] L. Lista[a],[52] D. Monorchio[ab],[52] G. Onorato[ab],[52] C. Sciacca[ab],[52] G. Raven,[53] H. L. Snoek,[53] C. P. Jessop,[54] K. J. Knoepfel,[54] J. M. LoSecco,[54] W. F. Wang,[54] G. Benelli,[55] L. A. Corwin,[55] K. Honscheid,[55] H. Kagan,[55] R. Kass,[55] J. P. Morris,[55] A. M. Rahimi,[55] J. J. Regensburger,[55] S. J. Sekula,[55] Q. K. Wong,[55] N. L. Blount,[56] J. Brau,[56] R. Frey,[56] O. Igonkina,[56] J. A. Kolb,[56] M. Lu,[56] R. Rahmat,[56] N. B. Sinev,[56] D. Strom,[56] J. Strube,[56] E. Torrence,[56] G. Castelli[ab],[57] N. Gagliardi[ab],[57]

Published in the Physical Review D

Work supported in part by US Department of Energy contract DE-AC02-76SF00515

M. Margoni[ab],[57] M. Morandin[a],[57] M. Posocco[a],[57] M. Rotondo[a],[57] F. Simonetto[ab],[57] R. Stroili[ab],[57] C. Voci[ab],[57] P. del Amo Sanchez,[58] E. Ben-Haim,[58] H. Briand,[58] G. Calderini,[58] J. Chauveau,[58] P. David,[58] L. Del Buono,[58] O. Hamon,[58] Ph. Leruste,[58] J. Ocariz,[58] A. Perez,[58] J. Prendki,[58] S. Sitt,[58] L. Gladney,[59] M. Biasini[ab],[60] R. Covarelli[ab],[60] E. Manoni[ab],[60] C. Angelini[ab],[61] G. Batignani[ab],[61] S. Bettarini[ab],[61] M. Carpinelli[ab],[61, ††] A. Cervelli[ab],[61] F. Forti[ab],[61] M. A. Giorgi[ab],[61] A. Lusiani[ac],[61] G. Marchiori[ab],[61] M. Morganti[ab],[61] N. Neri[ab],[61] E. Paoloni[ab],[61] G. Rizzo[ab],[61] J. J. Walsh[a],[61] D. Lopes Pegna,[62] C. Lu,[62] J. Olsen,[62] A. J. S. Smith,[62] A. V. Telnov,[62] F. Anulli[a],[63] E. Baracchini[ab],[63] G. Cavoto[a],[63] D. del Re[ab],[63] E. Di Marco[ab],[63] R. Faccini[ab],[63] F. Ferrarotto[a],[63] F. Ferroni[ab],[63] M. Gaspero[ab],[63] P. D. Jackson[a],[63] L. Li Gioi[a],[63] M. A. Mazzoni[a],[63] S. Morganti[a],[63] G. Piredda[a],[63] F. Polci[ab],[63] F. Renga[ab],[63] C. Voena[a],[63] M. Ebert,[64] T. Hartmann,[64] H. Schröder,[64] R. Waldi,[64] T. Adye,[65] B. Franek,[65] E. O. Olaiya,[65] F. F. Wilson,[65] S. Emery,[66] M. Escalier,[66] L. Esteve,[66] S. F. Ganzhur,[66] G. Hamel de Monchenault,[66] W. Kozanecki,[66] G. Vasseur,[66] Ch. Yèche,[66] M. Zito,[66] X. R. Chen,[67] H. Liu,[67] W. Park,[67] M. V. Purohit,[67] R. M. White,[67] J. R. Wilson,[67] M. T. Allen,[68] D. Aston,[68] R. Bartoldus,[68] P. Bechtle,[68] J. F. Benitez,[68] R. Cenci,[68] J. P. Coleman,[68] M. R. Convery,[68] J. C. Dingfelder,[68] J. Dorfan,[68] G. P. Dubois-Felsmann,[68] W. Dunwoodie,[68] R. C. Field,[68] A. M. Gabareen,[68] S. J. Gowdy,[68] M. T. Graham,[68] P. Grenier,[68] C. Hast,[68] W. R. Innes,[68] J. Kaminski,[68] M. H. Kelsey,[68] H. Kim,[68] P. Kim,[68] M. L. Kocian,[68] D. W. G. S. Leith,[68] S. Li,[68] B. Lindquist,[68] S. Luitz,[68] V. Luth,[68] H. L. Lynch,[68] D. B. MacFarlane,[68] H. Marsiske,[68] R. Messner,[68] D. R. Muller,[68] H. Neal,[68] S. Nelson,[68] C. P. O'Grady,[68] I. Ofte,[68] A. Perazzo,[68] M. Perl,[68] B. N. Ratcliff,[68] A. Roodman,[68] A. A. Salnikov,[68] R. H. Schindler,[68] J. Schwiening,[68] A. Snyder,[68] D. Su,[68] M. K. Sullivan,[68] K. Suzuki,[68] S. K. Swain,[68] J. M. Thompson,[68] J. Va'vra,[68] A. P. Wagner,[68] M. Weaver,[68] C. A. West,[68] W. J. Wisniewski,[68] M. Wittgen,[68] D. H. Wright,[68] H. W. Wulsin,[68] A. K. Yarritu,[68] K. Yi,[68] C. C. Young,[68] V. Ziegler,[68] P. R. Burchat,[69] A. J. Edwards,[69] S. A. Majewski,[69] T. S. Miyashita,[69] B. A. Petersen,[69] L. Wilden,[69] S. Ahmed,[70] M. S. Alam,[70] J. A. Ernst,[70] B. Pan,[70] M. A. Saeed,[70] S. B. Zain,[70] S. M. Spanier,[71] B. J. Wogsland,[71] R. Eckmann,[72] J. L. Ritchie,[72] A. M. Ruland,[72] C. J. Schilling,[72] R. F. Schwitters,[72] B. W. Drummond,[73] J. M. Izen,[73] X. C. Lou,[73] F. Bianchi[ab],[74] D. Gamba[ab],[74] M. Pelliccioni[ab],[74] M. Bomben[ab],[75] L. Bosisio[ab],[75] C. Cartaro[ab],[75] G. Della Ricca[ab],[75] L. Lanceri[ab],[75] L. Vitale[ab],[75] V. Azzolini,[76] N. Lopez-March,[76] F. Martinez-Vidal,[76] D. A. Milanes,[76] A. Oyanguren,[76] J. Albert,[77] Sw. Banerjee,[77] B. Bhuyan,[77] H. H. F. Choi,[77] K. Hamano,[77] R. Kowalewski,[77] M. J. Lewczuk,[77] I. M. Nugent,[77] J. M. Roney,[77] R. J. Sobie,[77] T. J. Gershon,[78] P. F. Harrison,[78] J. Ilic,[78] T. E. Latham,[78] G. B. Mohanty,[78] H. R. Band,[79] X. Chen,[79] S. Dasu,[79] K. T. Flood,[79] Y. Pan,[79] M. Pierini,[79] R. Prepost,[79] C. O. Vuosalo,[79] and S. L. Wu[79]

(The *BABAR* Collaboration)

[1]*Laboratoire de Physique des Particules, IN2P3/CNRS et Université de Savoie, F-74941 Annecy-Le-Vieux, France*
[2]*Universitat de Barcelona, Facultat de Fisica, Departament ECM, E-08028 Barcelona, Spain*
[3]*INFN Sezione di Bari[a]; Dipartmento di Fisica, Università di Bari[b], I-70126 Bari, Italy*
[4]*University of Bergen, Institute of Physics, N-5007 Bergen, Norway*
[5]*Lawrence Berkeley National Laboratory and University of California, Berkeley, California 94720, USA*
[6]*University of Birmingham, Birmingham, B15 2TT, United Kingdom*
[7]*Ruhr Universität Bochum, Institut für Experimentalphysik 1, D-44780 Bochum, Germany*
[8]*University of Bristol, Bristol BS8 1TL, United Kingdom*
[9]*University of British Columbia, Vancouver, British Columbia, Canada V6T 1Z1*
[10]*Brunel University, Uxbridge, Middlesex UB8 3PH, United Kingdom*
[11]*Budker Institute of Nuclear Physics, Novosibirsk 630090, Russia*
[12]*University of California at Irvine, Irvine, California 92697, USA*
[13]*University of California at Los Angeles, Los Angeles, California 90024, USA*
[14]*University of California at Riverside, Riverside, California 92521, USA*
[15]*University of California at San Diego, La Jolla, California 92093, USA*
[16]*University of California at Santa Barbara, Santa Barbara, California 93106, USA*
[17]*University of California at Santa Cruz, Institute for Particle Physics, Santa Cruz, California 95064, USA*
[18]*California Institute of Technology, Pasadena, California 91125, USA*
[19]*University of Cincinnati, Cincinnati, Ohio 45221, USA*
[20]*University of Colorado, Boulder, Colorado 80309, USA*
[21]*Colorado State University, Fort Collins, Colorado 80523, USA*
[22]*Technische Universität Dortmund, Fakultät Physik, D-44221 Dortmund, Germany*
[23]*Technische Universität Dresden, Institut für Kern- und Teilchenphysik, D-01062 Dresden, Germany*
[24]*Laboratoire Leprince-Ringuet, CNRS/IN2P3, Ecole Polytechnique, F-91128 Palaiseau, France*
[25]*University of Edinburgh, Edinburgh EH9 3JZ, United Kingdom*
[26]*INFN Sezione di Ferrara[a]; Dipartimento di Fisica, Università di Ferrara[b], I-44100 Ferrara, Italy*

[27]INFN Laboratori Nazionali di Frascati, I-00044 Frascati, Italy
[28]INFN Sezione di Genova[a]; Dipartimento di Fisica, Università di Genova[b], I-16146 Genova, Italy
[29]Harvard University, Cambridge, Massachusetts 02138, USA
[30]Universität Heidelberg, Physikalisches Institut, Philosophenweg 12, D-69120 Heidelberg, Germany
[31]Humboldt-Universität zu Berlin, Institut für Physik, Newtonstr. 15, D-12489 Berlin, Germany
[32]Imperial College London, London, SW7 2AZ, United Kingdom
[33]University of Iowa, Iowa City, Iowa 52242, USA
[34]Iowa State University, Ames, Iowa 50011-3160, USA
[35]Johns Hopkins University, Baltimore, Maryland 21218, USA
[36]Laboratoire de l'Accélérateur Linéaire, IN2P3/CNRS et Université Paris-Sud 11,
Centre Scientifique d'Orsay, B. P. 34, F-91898 Orsay Cedex, France
[37]Lawrence Livermore National Laboratory, Livermore, California 94550, USA
[38]University of Liverpool, Liverpool L69 7ZE, United Kingdom
[39]Queen Mary, University of London, London, E1 4NS, United Kingdom
[40]University of London, Royal Holloway and Bedford New College, Egham, Surrey TW20 0EX, United Kingdom
[41]University of Louisville, Louisville, Kentucky 40292, USA
[42]Johannes Gutenberg-Universität Mainz, Institut für Kernphysik, D-55099 Mainz, Germany
[43]University of Manchester, Manchester M13 9PL, United Kingdom
[44]University of Maryland, College Park, Maryland 20742, USA
[45]University of Massachusetts, Amherst, Massachusetts 01003, USA
[46]Massachusetts Institute of Technology, Laboratory for Nuclear Science, Cambridge, Massachusetts 02139, USA
[47]McGill University, Montréal, Québec, Canada H3A 2T8
[48]INFN Sezione di Milano[a]; Dipartimento di Fisica, Università di Milano[b], I-20133 Milano, Italy
[49]University of Mississippi, University, Mississippi 38677, USA
[50]Université de Montréal, Physique des Particules, Montréal, Québec, Canada H3C 3J7
[51]Mount Holyoke College, South Hadley, Massachusetts 01075, USA
[52]INFN Sezione di Napoli[a]; Dipartimento di Scienze Fisiche,
Università di Napoli Federico II[b], I-80126 Napoli, Italy
[53]NIKHEF, National Institute for Nuclear Physics and High Energy Physics, NL-1009 DB Amsterdam, The Netherlands
[54]University of Notre Dame, Notre Dame, Indiana 46556, USA
[55]Ohio State University, Columbus, Ohio 43210, USA
[56]University of Oregon, Eugene, Oregon 97403, USA
[57]INFN Sezione di Padova[a]; Dipartimento di Fisica, Università di Padova[b], I-35131 Padova, Italy
[58]Laboratoire de Physique Nucléaire et de Hautes Energies,
IN2P3/CNRS, Université Pierre et Marie Curie-Paris6,
Université Denis Diderot-Paris7, F-75252 Paris, France
[59]University of Pennsylvania, Philadelphia, Pennsylvania 19104, USA
[60]INFN Sezione di Perugia[a]; Dipartimento di Fisica, Università di Perugia[b], I-06100 Perugia, Italy
[61]INFN Sezione di Pisa[a]; Dipartimento di Fisica,
Università di Pisa[b]; Scuola Normale Superiore di Pisa[c], I-56127 Pisa, Italy
[62]Princeton University, Princeton, New Jersey 08544, USA
[63]INFN Sezione di Roma[a]; Dipartimento di Fisica,
Università di Roma La Sapienza[b], I-00185 Roma, Italy
[64]Universität Rostock, D-18051 Rostock, Germany
[65]Rutherford Appleton Laboratory, Chilton, Didcot, Oxon, OX11 0QX, United Kingdom
[66]CEA, Irfu, SPP, Centre de Saclay, F-91191 Gif-sur-Yvette, France
[67]University of South Carolina, Columbia, South Carolina 29208, USA
[68]Stanford Linear Accelerator Center, Stanford, California 94309, USA
[69]Stanford University, Stanford, California 94305-4060, USA
[70]State University of New York, Albany, New York 12222, USA
[71]University of Tennessee, Knoxville, Tennessee 37996, USA
[72]University of Texas at Austin, Austin, Texas 78712, USA
[73]University of Texas at Dallas, Richardson, Texas 75083, USA
[74]INFN Sezione di Torino[a]; Dipartimento di Fisica Sperimentale, Università di Torino[b], I-10125 Torino, Italy
[75]INFN Sezione di Trieste[a]; Dipartimento di Fisica, Università di Trieste[b], I-34127 Trieste, Italy
[76]IFIC, Universitat de Valencia-CSIC, E-46071 Valencia, Spain
[77]University of Victoria, Victoria, British Columbia, Canada V8W 3P6
[78]Department of Physics, University of Warwick, Coventry CV4 7AL, United Kingdom
[79]University of Wisconsin, Madison, Wisconsin 53706, USA

(Dated: August 14, 2008)

We present a measurement of the branching fractions for the Cabibbo-favored radiative decay, $D^0 \to \bar{K}^{*0}\gamma$, and the Cabibbo-suppressed radiative decay, $D^0 \to \phi\gamma$. These measurements are based on a data sample corresponding to an integrated luminosity of $387.1\,\text{fb}^{-1}$, recorded with the *BABAR* detector at the PEP-II e^+e^- asymmetric-energy collider operating at center-of-mass energies 10.58 and 10.54 GeV. We measure the branching fractions relative to the well-studied decay $D^0 \to K^-\pi^+$ and find $\mathcal{B}(D^0 \to \bar{K}^{*0}\gamma)/\mathcal{B}(D^0 \to K^-\pi^+) = (8.43 \pm 0.51 \pm 0.70) \times 10^{-3}$ and $\mathcal{B}(D^0 \to \phi\gamma)/\mathcal{B}(D^0 \to K^-\pi^+) = (7.15 \pm 0.78 \pm 0.69) \times 10^{-4}$, where the first error is statistical and the second is systematic. This is the first measurement of $\mathcal{B}(D^0 \to \bar{K}^{*0}\gamma)$.

PACS numbers: 13.25.Ft, 12.38.Qk, 12.40Vv, 11.30.Hv, 13.20.Fc

In the b-quark sector, radiative decay processes have provided a rich field in which to study the Standard Model of particle physics. Decays such as $B \to \rho\gamma$ have yielded measurements of the Cabibbo-Kobayashi-Maskawa matrix element $|V_{td}|$ [1, 2]. These decays are dominated by short-range electroweak processes, whereas long-range contributions are suppressed. The situation is reversed in the charm sector, where radiative decays are expected to be dominated largely by non-perturbative processes, examples of which are shown schematically in Fig. 1. Long-range contributions to radiative charm decays are expected to increase the branching fractions for these modes to values of the order of 10^{-5}, whereas short-range interactions are predicted to yield rates at the 10^{-8} level. Given the expected dominance of long-range processes, radiative charm decays provide a laboratory in which to test these QCD-based calculations.

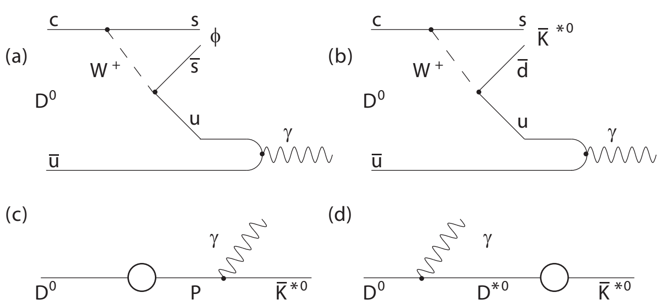

FIG. 1: Feynman diagrams for the long-range electromagnetic contributions to $D^0 \to V\gamma$, $V = \bar{K}^{*0}, \phi$. Figures (a) and (b) show sample vector dominance processes, while (c) and (d) are examples of pole diagrams, where the circles signify the weak transition and P represents a pseudoscalar meson.

Numerous theoretical models have been developed to describe these radiative charm decays [3–9]. The two most comprehensive studies [5, 9] predict very similar amplitudes for the dominant diagrams shown in Fig. 1. The first paper bases predictions on Vector Meson Dominance (VMD) calculations, while the second paper uses Heavy-Quark Effective Theory in conjunction with Chiral-Lagrangians. Though each approach arrives at similar estimates for the magnitudes of the individual decay amplitudes, Ref. [5] predicts that the pole diagrams, shown in Figs. 1 (c) and (d), interfere destructively and cancel nearly completely. Ref. [9] makes no such predictions. Precise measurements of $\mathcal{B}(D^0 \to V\gamma, V = \bar{K}^{*0}, \phi)$ may provide insight into the amount of interference between pole diagrams.

Mode	Experimental B.F. ($\times 10^{-5}$)	Theoretical[3–9] B.F. ($\times 10^{-5}$)
$D^0 \to \phi\gamma$	$(2.43^{+0.66}_{-0.57}(stat.)^{+0.12}_{-0.14}(sys.)$ [10]	$0.1 - 3.4$
$D^0 \to \bar{K}^{*0}\gamma$	< 76 (90% C.L.) [11]	$7 - 80$
$D^0 \to \rho^0\gamma$	< 24 (90% C.L.) [11]	$0.1 - 6.3$
$D^0 \to \omega\gamma$	< 24 (90% C.L.) [11]	$0.1 - 0.9$

TABLE I: The current experimental status and theoretical predictions for the branching fractions (B.F.) of radiative charm decays with vector mesons.

The first observation of a radiative, but color-suppressed, D^0 decay process was made by the Belle collaboration with a measurement of $\mathcal{B}(D^0 \to \phi\gamma) = (2.43^{+0.66}_{-0.57}(stat.)^{+0.12}_{-0.14}(sys.)) \times 10^{-5}$ [10]. CLEO II conducted searches for other radiative decays and established the current upper limit of $\mathcal{B}(D^0 \to \bar{K}^{*0}\gamma) < 7.6 \times 10^{-4}$ at 90% confidence level (C.L.), as well as upper limits on $\mathcal{B}(D^0 \to \rho^0\gamma)$ and $\mathcal{B}(D^0 \to \omega\gamma)$ [11]. Table I summarizes theoretical predictions and current experimental results.

In this paper we present the first observation of the Cabibbo-favored radiative decay $D^0 \to \bar{K}^{*0}\gamma$, as well as an improved branching fraction measurement of the previously observed decay $D^0 \to \phi\gamma$. The analysis is based on $387.1\,\text{fb}^{-1}$ of data recorded by the *BABAR* detector at the PEP-II e^+e^- asymmetric-energy collider operating at center-of-mass (CM) energies of $\sqrt{s} = 10.58$ GeV and 10.54 GeV, and uses approximately 5×10^8 $e^+e^- \to c\bar{c}$ events.

The *BABAR* detector is described in detail elsewhere [12]. Charged particle momenta are measured with a 5-layer double-sided silicon vertex tracker and a 40-layer drift chamber. Charged hadron identification is provided by measurements of the specific ionization energy loss, dE/dx, in the tracking system and of the Cherenkov angle obtained from a ring-imaging Cherenkov detector. An electromagnetic calorimeter consisting of 6580 CsI(Tl) crystals measures shower energy and position for electrons and photons. These detector elements are located inside, and coaxial with, the cryostat of a superconducting solenoidal magnet, which provides a 1.5 T magnetic field. The instrumented flux return of the magnet allows discrimination between muons and pions.

A detailed Monte Carlo (MC) simulation of the *BABAR* detector based on GEANT 4 [13] is used to validate the analysis and determine the reconstruction efficiencies.

We optimize our selection criteria using simulated events by maximizing significance, defined as $N_S/\sqrt{N_S+N_B}$, where N_S and N_B denote the number of signal and background candidates in the MC simulation. We reconstruct radiative $D^0 \to V\gamma$, $V = \bar{K}^{*0}, \phi$ decays using the charged decay modes of the vector meson, $\bar{K}^{*0} \to K^-\pi^+$ ($\phi \to K^-K^+$) [14]. We form $\bar{K}^{*0}$ (ϕ) candidates from pairs of oppositely charged tracks identified as $K^-\pi^+$ (K^-K^+) using the Cherenkov angle measurement of the DIRC and dE/dx measurements from the tracking system, and accept any $K^-\pi^+$ (K^-K^+) candidates with invariant mass in the range 0.848 to 0.951 GeV/c^2 (1.01 to 1.03 GeV/c^2). The charged track candidates are fit to a common vertex, and a fit probability greater than 0.1% is required.

A photon candidate is defined as an energy deposit in the EMC that is not associated with the trajectory of a charged track, and which exhibits the expected shower shape characteristics. Each such candidate is required to have CM energy greater than 0.54 GeV. The charged-particle vertex is assumed to be the production point of the photon. We suppress the significant background from $\pi^0 \to \gamma\gamma$ decays by rejecting a photon candidate which, when paired with another photon in the event, results in an invariant mass consistent with the π^0 mass, $(0.115 < M(\gamma\gamma) < 0.150)$ GeV/c^2.

Background from random $D^0 \to V\gamma$ candidates is reduced by requiring that the D^0 candidate be a product of the decay $D^{*+} \to D^0\pi^+$. A D^{*+} candidate is formed by combining a D^0 candidate with a low-momentum charged pion, denoted as π_s^+. These pion candidates are required to have CM momentum less than 450 MeV/c. We calculate the mass difference, $\Delta M = M(V\gamma\pi_s^+) - M(V\gamma)$ and require $(0.1435 < \Delta M < 0.1475)$ GeV/c^2. The ΔM distribution of candidates arising from signal decays is well-described by a Gaussian distribution function. Our selection corresponds to a six-standard deviation interval centered on the mean of the Gaussian, and hence retains almost all of the signal candidates. We reduce combinatoric background from $B\bar{B}$ events to a negligible level by requiring that the CM momentum of the D^{*+} candidate be greater than 2.62 GeV/c.

The dominant background in our sample of $D^0 \to \bar{K}^{*0}\gamma$ candidates results from $D^0 \to K^-\pi^+\pi^0$ decays, where one of the photons from the π^0 decay is paired with the kaon and pion from the D^0 decay to closely mimic the signal mode. As described above, we use a π^0 veto to suppress such events but, given the large branching fraction of this mode, $\mathcal{B}(D^0 \to K^-\pi^+\pi^0) = (13.5 \pm 0.6)\%$ [15], a significant number of such candidates survives. We can separate this background from signal on a statistical basis because of differences in the $K^-\pi^+\gamma$ invariant mass distribution. The background distribution peaks slightly below the nominal D^0 mass, and has a different shape from that of signal events. An additional background arises from $D^0 \to \bar{K}^{*0}\eta$ events where the η decays to two photons, one of which is combined with the $K^-\pi^+$ pair to form an invariant mass within our D^0 mass window. This contribution peaks well below the nominal D^0 mass, and it can be separated easily from correctly reconstructed $D^0 \to \bar{K}^{*0}\gamma$ decays.

The impact of both $D^0 \to \bar{K}^{*0}\pi^0$ and $D^0 \to \bar{K}^{*0}\eta$ is further reduced by using the $\bar{K}^{*0}$ helicity angle θ_H. The helicity angle is defined as the angle between the momentum of the $\bar{K}^{*0}$ meson parent particle (D^0) and the momentum of the $\bar{K}^{*0}$ daughter kaon as measured in the $\bar{K}^{*0}$ rest frame. Due to angular momentum conservation, $dN/d\cos\theta_H$ for signal candidates varies as $1 - \cos^2\theta_H$, whereas for $D^0 \to \bar{K}^{*0}\pi^0(\eta)$ events the cosine of the helicity angle is $\cos^2\theta_H$ distributed. The $\cos\theta_H$ distribution of $D^0 \to K^-\pi^+\pi^0$ candidates is complicated by the interference and overlap of resonant structure in the final state Dalitz plot. Based on a MC study an asymmetric selection of $-0.30 < \cos\theta_H < 0.65$ is chosen to maximize the signal significance.

Similarly, but to a lesser extent, the signal of the Cabibbo-suppressed radiative decay $D^0 \to \phi\gamma$ is obscured by backgrounds from $D^0 \to \phi\pi^0$ and $D^0 \to \phi\eta$ decays. Due to the small width of the ϕ meson, background from $D^0 \to K^-K^+\pi^0$ transitions with a K^+K^- invariant mass in the ϕ region yields a negligible contribution to $D^0 \to \phi\gamma$ [16]. Since angular momentum conservation dictates that the cosine of the helicity angle of the remaining $D^0 \to \phi\pi^0$ events follow a $\cos^2\theta_H$ distribution, we replace the tight $\cos\theta_H$ selection criterion used in the $D^0 \to \bar{K}^{*0}\gamma$ case with the looser requirement $|\cos\theta_H| < 0.9$ and include $\cos\theta_H$ as a variable in the fitting procedure. This retains a larger fraction of signal events, and so reduces statistical uncertainty.

We consider other radiative decays which might reflect into the $M(\bar{K}^{*0}\gamma)$ and $M(\phi\gamma)$ invariant mass distributions. Background to $D^0 \to \bar{K}^{*0}\gamma$ may arise from $D^0 \to \phi\gamma$ if a kaon from $\phi \to K^-K^+$ is mis-identified as a pion. Background from $D^0 \to \rho^0\gamma$ may arise if a pion from $\rho^0 \to \pi^-\pi^+$ is misidentified as a kaon. Real $D^0 \to \bar{K}^{*0}\gamma$ events can reflect into the $M(\phi\gamma)$ distributions if a π^+ is misidentified as a K^+. Using MC simulations, all of these background contributions are found to be negligible.

We extract the $D^0 \to \bar{K}^{*0}\gamma$ yield using an unbinned extended maximum likelihood method (E-MLM) to fit the $M(\bar{K}^{*0}\gamma)$ invariant mass spectrum. The yield of $D^0 \to \phi\gamma$ events is extracted using an E-MLM to fit the two dimensional distribution of invariant mass, $M(\phi\gamma)$, and helicity, $\cos\theta_H$.

We use a Crystal Ball (CB) line shape [17] to model the invariant mass distributions for $D^0 \to \bar{K}^{*0}\gamma$ ($D^0 \to \phi\gamma$) signal events, and background reflections from $D^0 \to K^-\pi^+\pi^0$ ($D^0 \to \phi\pi^0$) decays. The invariant mass distributions of $D^0 \to \bar{K}^{*0}\eta$ and $D^0 \to \phi\eta$ background events are modeled with a Gaussian function and a first order Chebychev polynomial. The remaining combinatoric background decays are modeled with a second order Chebychev polynomial. In the $\phi\gamma$, case the $\cos\theta_H$ distributions of $D^0 \to \phi\gamma$, $D^0 \to \phi\pi^0$, $D^0 \to \phi\eta$, and combinatoric background events are all modeled using second order Chebychev polynomials. The parameters of these probability distribution functions (PDFs) are obtained using simulated events and subsequently fixed when fitting the data.

We validate the invariant mass PDFs using data. To verify that the MC correctly simulates the backgrounds and the effects of the missing photon from the π^0 decay, we search our data sample for $D^0 \to K^0_S\gamma$ candidates. Since this decay is forbidden by angular momentum conservation, the candidates surviving our selection criteria are all combinatoric background or due to $D^0 \to K^0_S\pi^0$ or $D^0 \to K^0_S\eta$ decays.

We select K^0_S candidates from pairs of oppositely charged tracks identified as pions. The pions are required to share a common production vertex and have an invariant mass in the range $(0.490 < M(\pi^+\pi^-) < 0.505)\,\mathrm{GeV}/c^2$. Selection criteria for the photon momentum, D^{*+} momentum, ΔM, and π^0 veto are identical to those used in the $D^0 \to V\gamma$ analyses. The resulting $K^0_S\gamma$ invariant mass spectrum is fit with a linear combination of three PDFs. The first PDF is used to model $D^0 \to K^0_S\pi^0$ candidates, and has the same functional form as the one used to model $D^0 \to K^-\pi^+\pi^0$ candidates. The second PDF is used to model $D^0 \to K^0_S\eta$ candidates, and has the same functional form as that used to model $D^0 \to \bar{K}^{*0}\eta$ candidates. The third PDF is a second order Chebychev polynomial used to model combinatoric background candidates. The shapes for both $D^0 \to K^0_S\eta$ and combinatoric background candidates are fixed using MC. The $D^0 \to K^0_S\pi^0$ signal shape is allowed to float in the final fit. Both MC and data are fit in this way and we find good agreement. The observed differences in the fit parameters are used to correct the CB line shape PDFs as described below.

A second test is performed using $D^0 \to \bar{K}^{*0}\gamma$ candidates taken from the sideband regions defined by $|\cos\theta_H| > 0.9$. Very few $D^0 \to \bar{K}^{*0}\gamma$ candidates are seen within this region, leading to a clean sample of $D^0 \to K^-\pi^+\pi^0$ decays. The resulting D^0 invariant mass spectrum is fit using a procedure similar to the one used for signal region $D^0 \to \bar{K}^{*0}\gamma$ candidates. The only differences are that the $D^0 \to \bar{K}^{*0}\gamma$ contribution is fixed to zero, and the $D^0 \to K^-\pi^+\pi^0$ signal shape is allowed to float freely. The $M(\bar{K}^{*0}\gamma)$ distribution of $D^0 \to K^-\pi^+\pi^0$ events is compared between data and MC and we find good agreement.

Potential differences between the $D^0 \to V\gamma$ invariant mass distributions for data and MC are evaluated by using $D^0 \to K^0_S\pi^0$ events. The selection criteria for K^0_S mesons are identical to those applied in the $D^0 \to K^0_S\gamma$ analysis. The requirements on ΔM and D^{*+} CM momentum are as before. A π^0 candidate consists of a photon pair with invariant mass satisfying $(0.110 < M(\gamma\gamma) < 0.150)\,\mathrm{GeV}/c^2$, and resultant laboratory momentum greater than $0.540\,\mathrm{GeV}/c$. This resulting sample of $D^0 \to K^0_S\pi^0$ candidates is fit to a CB line shape and a linear background.

We used the average difference between the CB line shape parameters in MC and these data control samples to modify the PDF parameterizations used in the fit.

The fit results from data and expected signal and background contributions from MC are shown in Fig. 2(a-c). The event yields obtained from the E-MLM fit for both $D^0 \to \phi\gamma$ and $D^0 \to \bar{K}^{*0}\gamma$ are $N(D^0 \to \phi\gamma;\ \phi \to K^-K^+) = 242.6 \pm 24.8$ and $N(D^0 \to \bar{K}^{*0}\gamma;\ \bar{K}^{*0} \to K^-\pi^+) = 2285.8 \pm 113.2$. The reconstruction efficiencies, determined using MC, are found to be $\epsilon(D^0 \to \phi\gamma;\ \phi \to K^-K^+) = (10.8 \pm 0.1)\%$ and $\epsilon(D^0 \to \bar{K}^{*0}\gamma;\ \bar{K}^{*0} \to K^-\pi^+) = (6.4 \pm 0.1)\%$.

In order to avoid uncertainties in the overall normalization we measure the branching fraction of the radiative decays relative to $\mathcal{B}(D^0 \to K^-\pi^+)$. We prepare a $D^0 \to K^-\pi^+$ dataset following procedures similar to those described above, and find a yield $N(D^0 \to K^-\pi^+) = (335.1 \pm 4.0) \times 10^3$ with an efficiency of $\epsilon(D^0 \to K^-\pi^+) = (5.3 \pm 0.2)\%$.

We perform several consistency checks. Our result is compared to the $\cos\theta_H$ distribution expected for $D^0 \to \bar{K}^{*0}\gamma$ by refitting the data in intervals of $\cos\theta_H$ and measuring $N(D^0 \to \bar{K}^{*0}\gamma)$ in each interval. The normalized and efficiency-corrected result, shown in Fig. 2(d), compares well to the expected distribution. As an additional check, we divide the data into five distinct samples, one for each PEP-II run period, and perform the analysis on each subset independently. We see a $D^0 \to \bar{K}^{*0}\gamma$ signal for each run period, and find that the branching ratios are consistent within statistical uncertainties.

We evaluate the systematic uncertainties associated with our measurement in several different studies. Systematic effects due to the PDF parameterizations of signal and backgrounds are determined by generating an ensemble of 1,000 random numbers drawn from a normal distribution for each PDF parameter, including their correlations obtained from our fits. We refit the data using each of the $1,000$ sets of random numbers. The resulting distribution of $N(D^0 \to V\gamma)$ is fit to a Gaussian function and the percent standard deviation is taken as the systematic error, 5.9% for $D^0 \to \phi\gamma$ and 4.4% for $D^0 \to \bar{K}^{*0}\gamma$.

Correcting the $D^0 \to V\gamma$ and $D^0 \to V\pi^0$ PDF parameters using the data control samples induces a second systematic uncertainty in the parameterization of the signal shapes. We estimate this effect by independently applying the corrections obtained using each of the three control samples. The largest percentage variation in $N(D^0 \to V\gamma)$ is taken as the systematic uncertainty associated with this correction; this leads to systematic uncertainities of 3.0% for $N(D^0 \to \phi\gamma)$ and 4.3% for

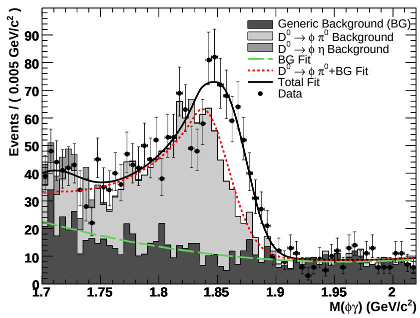

(a) The $\phi\gamma$ invariant mass distribution.

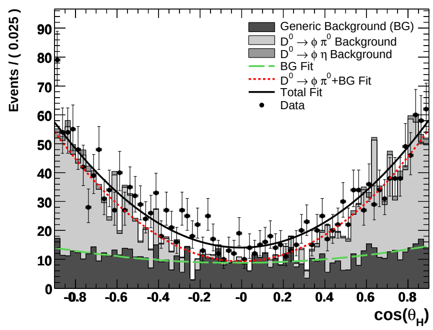

(b) The $\phi\gamma$ helicity angle distribution.

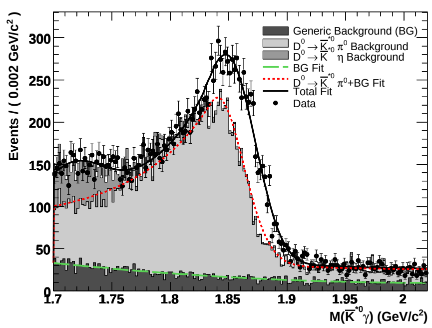

(c) The $\bar{K}^{*0}\gamma$ invariant mass distribution.

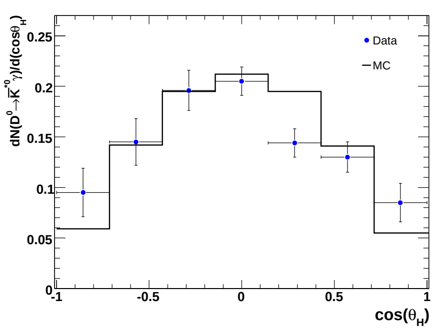

(d) The $D^0 \to \bar{K}^{*0}\gamma$ helicity angle distribution.

FIG. 2: Invariant mass and $\cos\theta_H$ distributions for data (points) and simulated events (histograms). The curves show the fit results and the individual signal and background contributions. BG refers to the combinatoric background.

$N(D^0 \to \bar{K}^{*0}\gamma)$.

We quantify the difference in particle identification (PID) efficiency between data and simulation by means of a high-purity control sample of $D^{*+} \to D^0\pi^+$, $D^0 \to K^-\pi^+$ events, which we divide into intervals of polar angle and momentum. The change in yield when PID selection criteria are applied is computed separately for data and for simulated events and the difference is taken as a correction factor for that interval. We then weight the correction factors according to the expected momentum and polar-angle distributions of the $D^0 \to \bar{K}^{*0}\gamma$ signal. While a portion of the PID systematic uncertainty for our signal modes is canceled when measuring the branching fractions in ratio to $D^0 \to K^-\pi^+$, the residual uncertainty is found to be 2.88% for $D^0 \to \phi\gamma$ and 1.10% for $D^0 \to \bar{K}^{*0}\gamma$. By measuring $\mathcal{B}(D^0 \to \bar{K}^{*0}\gamma)$ and $\mathcal{B}(D^0 \to \phi\gamma)$ with respect to $D^0 \to K^-\pi^+$, first-order effects from charged particle tracking also cancel, leaving only a second order systematic uncertainty of 1.00% for $D^0 \to \bar{K}^{*0}\gamma$ events and 1.20% for $D^0 \to \phi\gamma$. We summarize all systematic uncertainties in Table II.

Systematic	$\sigma(D^0 \to \phi\gamma)$ (%)	$\sigma(D^0 \to \bar{K}^{*0}\gamma)$ (%)
Tracking, vertexing	1.2	1.0
Particle ID	2.9	1.1
γ reconstruction	1.8	1.8
π^0 veto	1.8	1.8
PDF parameter	5.9	4.4
Correcting $\mathcal{P}_{D^0\to V\gamma}$ and $\mathcal{P}_{D^0\to V\pi^0}$	3.0	4.3
Ref. mode efficiency	1.5	1.5
Selection criteria	5.4	4.5
Total systematic effect	9.6	8.3

TABLE II: Summary of all systematic errors for each D^0 decay mode. The total systematic uncertainty is obtained by adding the individual systematic estimates in quadrature.

In this paper, we report our observation of the Cabibbo-favored, but color-suppressed, radiative decay $D^0 \to \bar{K}^{*0}\gamma$. We also present confirmation of the previous measurement of the Cabibbo-suppressed radiative decay $\mathcal{B}(D^0 \to \phi\gamma)$, but with reduced statistical uncertainities. The measured branching ratios are

$$\frac{\mathcal{B}(D^0 \to \phi\gamma)}{\mathcal{B}(D^0 \to K^-\pi^+)} = (7.15 \pm 0.78 \pm 0.69) \times 10^{-4}$$
$$\frac{\mathcal{B}(D^0 \to \bar{K}^{*0}\gamma)}{\mathcal{B}(D^0 \to K^-\pi^+)} = (8.43 \pm 0.51 \pm 0.70) \times 10^{-3}$$

where the first uncertainty is statistical and the second is systematic. Using the current world average of $\mathcal{B}(D^0 \to K^-\pi^+) = (3.82 \pm 0.07)\%$ [15] we obtain the following absolute branching fractions:

$$\mathcal{B}(D^0 \to \phi\gamma) = (2.73 \pm 0.30 \pm 0.26) \times 10^{-5}$$
$$\mathcal{B}(D^0 \to \bar{K}^{*0}\gamma) = (3.22 \pm 0.20 \pm 0.27) \times 10^{-4}.$$

These results are consistent with the theoretical expectations of Table I.

In the context of the vector dominance model the largest contribution to radiative D^0 decays is expected to come from a virtual ρ^0 coupling directly to a single photon, leading to the prediction that the branching ratios $\mathcal{B}(D^0 \to \phi\gamma)/\mathcal{B}(D^0 \to \bar{K}^{*0}\gamma)$ and $\mathcal{B}(D^0 \to \phi\rho^0)/\mathcal{B}(D^0 \to \bar{K}^{*0}\rho^0)$ should be equal [5]. Comparing our measurements of the radiative D^0 decays with the current world averages [15] we find

$$\frac{\mathcal{B}(D^0 \to \phi\gamma)}{\mathcal{B}(D^0 \to \bar{K}^{*0}\gamma)} = (6.27 \pm 0.71 \pm 0.79) \times 10^{-2}$$

$$\frac{\mathcal{B}(D^0 \to \phi\rho^0)}{\mathcal{B}(D^0 \to \bar{K}^{*0}\rho^0)} = (6.7 \pm 1.6) \times 10^{-2}$$

in agreement with this prediction.

If we assume all contributions are from VMD type processes and under the assumption that the ρ^0 meson is transversely polarized, as has been confirmed experimentally for $D^0 \to \bar{K}^{*0}\rho^0$ [15], we expect $\mathcal{B}(D^0 \to V\gamma) \approx \alpha_{EM}\mathcal{B}(D^0 \to V\rho^0)$ [5], where $\alpha_{EM} = 1/137$ is the fine structure constant. Using our results we find

$$\mathcal{B}(D^0 \to \bar{K}^{*0}\gamma) = (0.021 \pm 0.005)\, \mathcal{B}(D^0 \to \bar{K}^{*0}\rho^0)$$
$$\mathcal{B}(D^0 \to \phi\gamma) = (0.020 \pm 0.003)\, \mathcal{B}(D^0 \to \phi\rho^0)$$

which in both cases is about a factor of three larger than the VMD prediction. This indicates that we are seeing enhancements from processes other than VMD, which might be explained by incomplete cancellation between pole diagrams.

We are grateful for the excellent luminosity and machine conditions provided by our PEP-II colleagues, and for the substantial dedicated effort from the computing organizations that support *BaBar*. The collaborating institutions wish to thank SLAC for its support and kind hospitality. This work is supported by DOE and NSF (USA), NSERC (Canada), CEA and CNRS-IN2P3 (France), BMBF and DFG (Germany), INFN (Italy), FOM (The Netherlands), NFR (Norway), MES (Russia), MEC (Spain), and STFC (United Kingdom). Individuals have received support from the Marie Curie EIF (European Union) and the A. P. Sloan Foundation.

---

* Deceased
† Now at Temple University, Philadelphia, Pennsylvania 19122, USA
‡ Now at Tel Aviv University, Tel Aviv, 69978, Israel
§ Also with Università di Perugia, Dipartimento di Fisica, Perugia, Italy
¶ Also with Università di Roma La Sapienza, I-00185 Roma, Italy
** Now at University of South Alabama, Mobile, Alabama 36688, USA
†† Also with Università di Sassari, Sassari, Italy

[1] A. Ali and A. Y. Parkhomenko, Eur. Phys. J. **C23**, 89 (2002).
[2] A. Ali, E. Lunghi, and A. Y. Parkhomenko, Phys. Lett. **B595**, 323 (2004).
[3] B. Bajc, S. Fajfer, and R. J. Oakes, Phys. Rev. **D51**, 2230 (1995).
[4] B. Bajc, S. Fajfer, and R. J. Oakes, Phys. Rev. **D54**, 5883 (1996).
[5] G. Burdman, E. Golowich, J. L. Hewett, and S. Pakvasa, Phys. Rev. **D52**, 6383 (1995).
[6] H.-Y. Cheng et al., Phys. Rev. **D51**, 1199 (1995).
[7] S. Fajfer, A. Prapotnik, S. Prelovsek, P. Singer, and J. Zupan, Nucl. Phys. Proc. Suppl. **115**, 93 (2003).
[8] S. Fajfer and P. Singer, Phys. Rev. **D56**, 4302 (1997).
[9] S. Fajfer, S. Prelovsek, and P. Singer, Eur. Phys. J. **C6**, 471 (1999).
[10] K. Abe *et al.*, Phys. Rev. Lett. **92**, 101803 (2004), the published result has been rescaled using the latest values from [15].
[11] D. M. Asner *et al.*, Phys. Rev. **D58**, 092001 (1998).
[12] B. Aubert *et al.*, Nucl. Instrum. Meth. **A479**, 1 (2002).
[13] S. Agostinelli et al., Nucl. Instrum. Meth. **A506**, 250 (2003).
[14] Unless explicitly stated otherwise, charge conjugate reactions are included throughout this paper.
[15] W.-M. Yao *et al.* (Particle Data Group), J. Phys. **G33**, 1 (2006), and 2007 partial update for the 2008 edition.
[16] B. Aubert *et al.*, Phys. Rev. **D76**, 011102 (2007).
[17] M. J. Oreglia, Ph.D Thesis, SLAC-236 (1980), J. E. Gaiser, Ph.D. Thesis, SLAC-255 (1982), T. Skwarnicki, Ph.D Thesis, DESY F31-86-02 (1986).